

A REFERENCE MEASUREMENT SYSTEM FOR ELECTROSHOCK WEAPONS

Nicholas G. Paulter, Jr. and Donald R. Larson

National Institute of Standards and Technology

100 Bureau Drive, Gaithersburg, MD 20899-8102

Abstract

We have developed a measurement system to measure accurately the electrical current and high-voltage output of an electroshock weapon (ESW) that is used to deliver an electrical stimulus to humans for the purpose of incapacitation. Since the outputs of several ESWs consist of a train of impulse-like signals having transients with a duration of 10 ns or less and pulse train duration greater than 5 s, we have assembled a unique waveform recorder, using commercially-available components, to acquire this time varying output of the ESW.

The electrical load needed to simulate the load presented by the human body (the target) will also be discussed. We have developed a variable load that can be automatically changed between pulses from an ESW. The pulse parameters selected for measurement are discussed. An uncertainty analysis of the measurement system and measurement results has been developed and are presented.

We will also report on the progress of IEC62792 “Electroshock weapon measurement method,” a standard being developed by Working Group 22 of the IEC TC 85.

Key Words: electroshock weapon, measurement uncertainty, standard, waveform recorder

Introduction

Electroshock weapons are electronic devices designed to incapacitate a human using electrical energy. The ESWs that we consider are those that shoot barbed darts into the target, where these darts are electrically connected to the ESW body by wire tethers. Since an ESW is intended to apply only a less-than-lethal, high voltage electrical waveform to a human, it is vitally important to accurately measure this waveform. The standard should indicate which waveform parameters may be important in characterizing an ESW and the best practices for measuring these parameters. The work presented here describes a measurement system that can accurately and reproducibly measure the electrical outputs of an ESW.

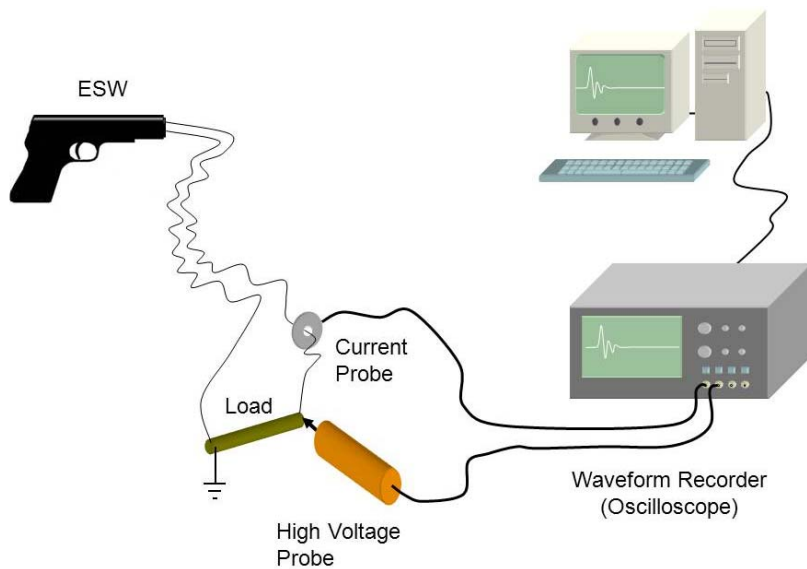


Figure 1. Measurement system.

important alternative to human subject testing. A knowledge of the voltage and current as a function of time allows the calculation of the energy applied by an ESW.

Choice of Parameters

The medical literature (see [1] and [2] for examples) indicates that the current, energy, and waveform shape are waveform parameters important to the efficacy and safety of an ESW. IEC Standard 60479-2 addresses the threshold level for fibrillation of several current waveforms applied to humans [3]. Therefore, we have focused our efforts to ensure accurate and reliable measurements of the current and voltage waveforms, where we compute energy from the current and voltage. The medical literature also indicates that the load impedance the ESW must drive may also vary widely. This load impedance is not fixed and varies with both voltage and frequency [4].

Measurement System

We use a waveform recorder to measure the output of an ESW as a function of time. Since the high voltage output of an ESW would immediately damage the input of most waveform recorders, voltage and current probes are used. Our measurement system consists of a programmable resistive load, a voltage probe, a current probe, and a waveform recorder (figure 1).

We have chosen to measure ESW output using a waveform recorder to capture the amplitude of the voltage and current, each independent of the other, as a function of time. Using a resistive electrical load to simulate the load a human provides is an

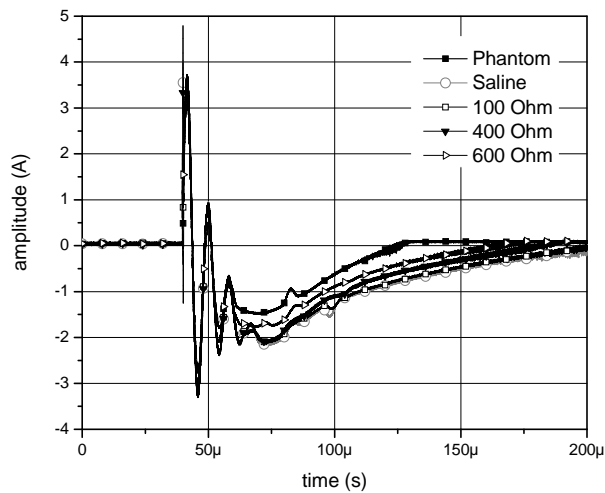


Figure 2. Current waveforms for various loads. used in tests of ESWs [6, 7].

Load

Testing of ESWs requires a resistive electrical load to simulate the resistance of the human body, which is typically that of the torso of an adult human male.

Selection of a load is complicated by research that indicates human tissue may change resistance if subjected to high voltages in the range generated by ESWs [5]. A literature search reveals that several different resistive loads have been

We have performed measurements using several different loads. Some measurements were made using a human phantom material consisting of a carbon black loaded fluoroelastomer, which emulates the average impedance of the human body over a frequency range of approximately 100 Hz to 1 MHz [8]. Measurements were also performed using a normal saline solution (nominally 0.9 % weight per volume) as the load. Measurements were made using a variety of commercial, non-inductive, high voltage resistors. A resistor with a nominal resistance of 100 Ω was used in our initial measurements based on the literature previously cited. Resistors with nominal resistance values of 400 Ω and 600 Ω were used to allow comparison with the measurement results of others [9]. The 100 Ω resistor and the saline solution gave nearly identical results (figure 2).

Although the open-circuit output of an ESW may exceed 50 kV, the voltage produced under load is significantly less; a value of approximately 5 kV has been reported using a 400 Ω load [6]. We have designed a programmable load circuit that allows the load to be changed quickly between pulses contained within the pulse train generated by a single activation of an ESW. Since the output may exceed 50 kV if there is no load, the variable load circuit was designed to provide a load of 1000 Ω when switching between one load resistor and another. The circuit uses high voltage relays designed to switch up to 15 kV in about 3 ms. The load resistors are low inductance, high voltage resistors rated for about 9 kV and 3.25 W. Using this variable load circuit, we have observed that the output voltage of the ESW changes

significantly when the load is changed but that the amplitude of the current is relatively unchanged (figure 2). This indicates that the ESW acts as a current source for these load conditions.

Current and Voltage Probes

The current is measured using a wide-band current probe that consists of a current transformer with a coaxial output connector. The ESW wire conducting its output to a dart is passed through the center of the current transformer. The current transformer provides a voltage output that is used to compute the current through the wire. The specification for the current/voltage conversion ratio for the probes we use is approximately 1 A/V. Other pertinent characteristics of this probe are: 3 dB attenuation bandwidth of about 300 Hz at the low frequency cut-off and about 200 MHz at the high frequency cut-off, step response of about 1.5 ns, and an output impedance of 50 Ω .

The voltage is measured using a resistive/capacitive voltage divider with a nominal input to output voltage ratio of 2000:1. Its 3 dB attenuation bandwidth is dc to about 110 MHz, which is equivalent to a step response of about 3.2 ns, an input resistance of about 400 M Ω in parallel with 10 pF capacitor, and an output impedance designed to be connected to a 1 M Ω load.

Characterization of Voltage Probe Transfer Function

The transfer function of the voltage probe was characterized by comparing measurements made with and without the voltage probe. A programmable pulse source capable of generating pulses with selectable amplitude and pulse/step duration was used. Different nominal pulse durations were selected, 10 ns, 20 ns, 200 ns, and 400 ns. The amplitude was fixed at approximately 70 V. These pulses were measured and the ratio of the amplitudes compared. The 10 ns pulse was distorted slightly by the bandwidth limitations of the probe. For pulse durations greater than 10 ns, the pulse exhibited significant overshoot that also made determining the pulse amplitude difficult. Since the 400 ns pulse waveform contained a well-defined high state after the overshoot, it was used to obtain the input to output voltage ratio. The ratio of the amplitudes was 1817.9 ± 0.2 (all reported uncertainties are equal to the expanded uncertainty with a coverage factor of two unless otherwise noted). The 3 dB attenuation bandwidth of the probe was determined using the spectra of the waveforms taken

with and without the probe, which was determined to be $59.8 \text{ MHz} \pm 0.4 \text{ MHz}$ (this uncertainty is the standard deviation of repeated measurements) and the step response transition duration (10 % to 90 % of pulse amplitude) was $5.0 \text{ ns} \pm 0.1 \text{ ns}$. The accuracy of this process is dependent on the gain linearity of the waveform recorder and the difference in amplitude of the two signals used to calculate the probe transfer function. To reduce this difference from a factor of nearly 2000 to about 200, we used a high bandwidth, calibrated 20 dB attenuator. The waveform recorder input channel is digitized using an 8 bit analog-to-digital converter (ADC), for which the manufacturer claims its linearity is better than 1 LSB. This is examined in more detail in the section “Oscilloscope gain error or linearity”.

In addition to the time-domain measurements, we performed a swept frequency measurement of the voltage probe transfer function. This was done using a sine wave signal generator connected to the oscilloscope with and without the high voltage probe. The oscilloscope was used to determine the amplitude of the sine wave in both cases.

The manufacturer’s calibration of the voltage probe indicates that the 2000:1 voltage ratio has an uncertainty of $\pm 1 \%$ for frequencies under 200Hz, $\pm 1.5 \%$ for frequencies under 5 MHz, and $\pm 5 \%$ for frequencies greater than 5 MHz (to the limit of 110 MHz). Our time-domain and frequency-domain testing found the ratio to be 1818:1 over nearly the entire frequency range, a difference of 9 % from the manufacturer’s specification.

Characterization of Current Probe Transfer Function

The current probe converts the current to a voltage using a hollow coil through which the signal wire passes. The current probe was characterized by measuring the voltage amplitude of the applied waveform, measuring the load resistance, calculating the current, and comparing the calculated current to the measured output of the current probe. An impulse-like signal with a pulse duration of nominally 100 ns from an arbitrary function generator (25 MHz BW) was measured using the oscilloscope. At the same time, the output of the current probe was also measured using the oscilloscope. The input resistance of the oscilloscope input was measured using a digital ohmmeter. The measured voltage waveform was divided by the measured resistance and compared to the measured current waveform. We determined the conversion factor, frequency response, and transition duration of the probe by using an oscilloscope to measure the current resulting from the application of a

known impulse. The manufacturer's provided conversion factor and bandwidth compared well with our determination: we measured the conversion factor to be $0.999 \text{ A/V} \pm 0.002 \text{ A/V}$. The 3 dB attenuation bandwidth was determined to be $196.4 \text{ MHz} \pm 0.3 \text{ MHz}$ (this uncertainty is the standard deviation of repeated measurements) and the step response transition duration was $1.71 \text{ ns} \pm 0.02 \text{ ns}$. This is comparable to the manufacturer's specification of 300 Hz to 200 MHz.

Waveform Recorders

The waveform recorder has stringent performance requirements: approximate time resolution of 1 ns, 3 dB attenuation bandwidth greater than 1 GHz, waveform epoch up to 12 s, amplitude resolution of at least 8 bits, and signal-to-noise ratio greater than 40 dB. To achieve these requirements we assembled a waveform recorder using three high memory capacity data capture boards linked together. With this configuration we have a system with sufficient memory to capture 12 seconds of data with a time resolution of 1 ns. In operation the signal is split three ways and connected to each of the three data acquisition boards. The first board is triggered by the waveform to be measured, and the next board is triggered when the previous board finishes its commanded acquisition. We used a commercial-off-the-shelf (COTS) digital oscilloscope to establish the calibration process for the measurement system and to develop the performance requirements for our custom system. The COTS oscilloscope operates and functions identically to the custom system we developed but has insufficient memory.

Characterization of the Oscilloscope

The COTS oscilloscope employed in this study was always operated in a "real-time mode." In this mode the oscilloscope is always acquiring a signal input; when a trigger signal is received the oscilloscope captures and displays the acquired waveform.

Waveform recorder impulse response

A step-like pulse with a transition duration of about 15 ps was used to determine the bandwidth of the waveform recorder. The manufacturer's data indicates that the COTS oscilloscope bandwidth is 500 MHz. We measured a 3 dB attenuation bandwidth of $567.2 \text{ MHz} \pm 2.6 \text{ MHz}$ (this uncertainty is the standard deviation of repeated measurements).

Oscilloscope transient gain

“A common practice in oscilloscope calibrations is to use or include a static level gain-correction” [10]. However, since the signals being measured are impulses, as opposed to static levels, a transient gain term should be used. “The transient gain is affected by the impulse response of the sampler” [10]. The transient gain was measured by applying the output of a calibrated reference step generator to the oscilloscope and comparing the measured amplitude to the input amplitude. The amplitude of the reference step generator was obtained using the NIST Sampling Waveform Analyzer [11]. The transient gain was determined to be $1.01 \text{ V/V} \pm 0.001 \text{ V/V}$ for both channel 1 and channel 2 of the COTS oscilloscope.

Oscilloscope gain error or linearity

The linearity of the oscilloscope is critical to determining the voltage probe divider ratio. The linearity of the oscilloscope was determined by applying 125 kHz sine waves that varied between the minimum and maximum amplitudes used in determining the voltage probe divider ratio (0.01 V to 3.16 V). This frequency was chosen because it is the approximate repetition rate of the positive and negative transients that comprise each pulse from an ESW. The amplitudes of these sine waves were also measured using a calibrated RF power meter. A line fit to the measured amplitude data exhibited a mean square error of $3.8 \times 10^{-4} \text{ V/V}$.

Timebase calibration

The oscilloscope timebase must be calibrated to ensure the digitizing interval is known and uniform. If not, these errors may have to be corrected and/or appropriate uncertainties attributed to the temporal information of the waveforms. The timebase error, $u_{\Delta t}$, was measured using known sine wave signals in a method described in [12]. In a 200 μs epoch (duration of one pulse), the maximum error in a sample instant was about $\pm 32.9 \text{ ns}$, and the mean was $0.8 \text{ ns} \pm 6.8 \text{ ns}$. This is a maximum error of approximately 165 parts per million and an order of magnitude greater than the manufacturer’s claimed timebase accuracy of 15 parts per million. This uncertainty contributes to the voltage and current pulse duration measurement results and to the energy calculations.

Factors Effecting Measurements

Our goal is to measure the parameters of the signal applied to the load and the associated measurement uncertainty of those parameters. Determination of the “ideal” load impedance for testing ESWs will be the subject of another study. The measured waveforms, $w_{meas}(t)$, recorded by the waveform recorder are a convolution of the input signal, $s_{in}(t)$, the transfer function of the voltage or current probe, $h_{probe}(t)$, and the impulse response of the waveform recorder, $h_{scope}(t)$. In (1), the asterisk represents the convolution function.

$$w_{meas}(t) = s_{in}(t) * h_{probe}(t) * h_{scope}(t) \quad (1)$$

Convolution in the time domain is equivalent to multiplication of spectra in the frequency domain:

$$W_{meas}(f) = S_{in}(f) \times H_{probe}(f) \times H_{scope}(f) \quad (2)$$

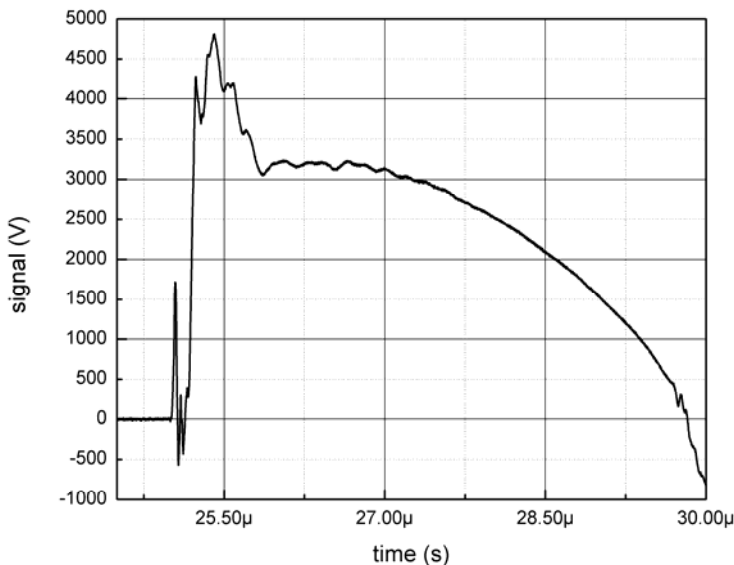
Solving (2) for $S_{in}(f)$ results in:

$$S_{in}(f) = \frac{W_{meas}(f)}{H_{probe}(f) \times H_{scope}(f)} \quad (3)$$

Calculating the inverse Fourier transform of $S_{in}(f)$ yields the input signal applied to the load, $s_{in}(t)$. Since deconvolution in the presence of noise is an ill-posed problem, great care must be exercised in implementing this process and interpreting its results.

Electroshock Weapon Measurement Results

The current and voltage signal from an ESW applied to the human phantom load was measured and recorded. The positive interval of a single ESW voltage pulse waveform is depicted in figure 3. The amplitude of the initial spike is nearly 4800 Volts but quickly drops



to a value of approximately 3100 Volts. The duration of the initial positive pulse is approximately 3.8 μ s (duration at the 50 % reference level instants). The waveform transitions to a negative pulse with an amplitude of approximately -2500 Volts and has a duration

Figure 3. Expanded display of first voltage pulse transition.

of approximately 4 μs . After the initial positive and negative pulses, the waveform continues to ring and exhibits several more positive and negative pulses with a slow decay to the base state. The duration of this complex waveform is approximately 125 μs . For this particular ESW, these waveforms are repeated approximately 92 times during a 5 second interval after each trigger pull.

The frequency spectrum from a waveform captured by the current probe is depicted in figure 4 (effects of the current probe's impulse response were not removed). The peak at 103 kHz is due to the large oscillations seen in figure 4. Although the 3 dB attenuation bandwidth for the ESW output is approximately 8 kHz, frequencies to 5 MHz contain significant energy.

As previously stated, for each shot, that is, each time the trigger is pulled, the ESW we tested outputs a series of approximately 92 pulses during a nearly 5 second interval. However, the

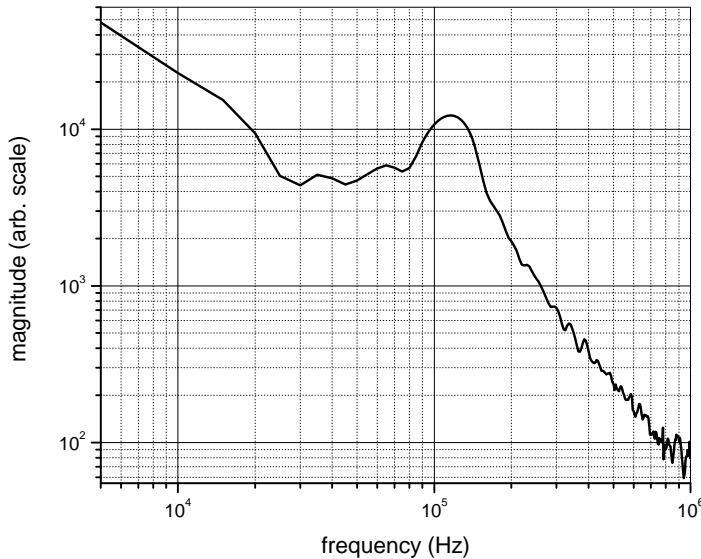


Figure 4. Frequency spectrum of current pulse.

ESW does not always generate the same number of pulses each time it is fired even if the load is the same and the battery is fresh. The manufacturer states that the battery is good for 100 shots. For the first 100 shots, starting with a fresh battery, the number of pulses measured with each shot had a mean of 91.2 pulses \pm 1.7 pulses and ranged from a maximum of 92 and a minimum of 87.

Additional shots were made until the battery was depleted (figure 5). The recorded waveform had a 10 second epoch and a time resolution of 2.5 μs . This is less than the duration of the initial positive pulse and much less than the 125 μs complex structured waveform. It is highly unlikely that a pulse was missed in the recorded waveform due to insufficient time resolution.

For the first 100 shots depicted in figure 5, the average pulse spacing between the first two pulses is approximately $52.9 \text{ ms} \pm 1 \text{ ms}$ and the spacing between the last two pulses is approximately $55.5 \text{ ms} \pm 1 \text{ ms}$. The average pulse spacing is $54.5 \text{ ms} \pm 1 \text{ ms}$.

Since the number of pulses generated in each shot is not a constant, it may be anticipated that the characteristics of the pulses generated may be dependent on the number of pulses per shot. However, an examination of the amplitude voltage and the standard deviation of the amplitude voltage as a function of the number of shots did not reveal a change in amplitude when the number of pulses varied from 78 to 92.

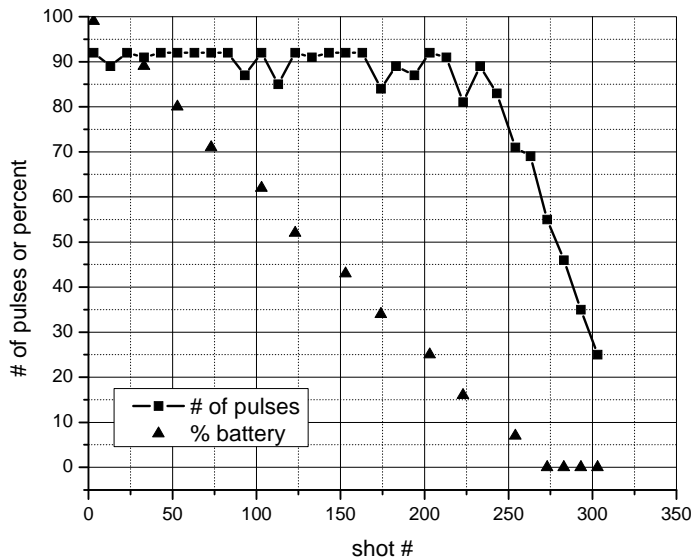


Figure 5. Pulse count and reported battery life.

Uncertainty Analysis

The electrical pulse generated by the ESW has a complex structure that reflects plasma formation or the break-down process (figure 2) that occurs in the spark gap. It may be referred to as a “lightning impulse,” a waveform described in the IEEE Std 4-1995 “IEEE Standard Techniques for High-Voltage Testing” [13], for which it states that “no general guidance

can be given for the determination of the value of the test voltage.” However, the signals generated by the ESW can be considered to be a series of pulses, both positive and negative. Therefore, the uncertainty analysis used follows the pulse parameter uncertainty analysis described in [10]. The average of each parameter W , is obtained from a set of M_1 measured pulse waveforms and each parameter is dependent on a number of variables α_j (see equation 2 in [10]).

$$u_{\bar{W}} = k_{eff} \sqrt{\frac{1}{M_1} \sum_j \left(\frac{\partial W_i(\alpha_j)}{\partial \alpha_j} \right)^2 u_j^2} \quad (4)$$

Equation 4 assumes that each of the variables α_j are uncorrelated. The term k_{eff} is the effective degrees of freedom or a statistical weighting term and u_j is the uncertainty in the j^{th} variable for the parameter W .

IEC draft Standard 62792

The IEC draft standard 62792, “Electroshock weapon measurement method,” is being written by the IEC Technical Committee (TC) 85, “Measuring equipment for electrical and electromagnetic properties,” Project Team 62792. The project team comprises members from the Russian Federation, Japan, China, Canada, and the USA. The project was initiated in March 2012.

The draft standard is written as a measurement method standard and not as a performance requirement for ESWs, which would require accurate and reliable knowledge on the limitations for both safety and efficacy of the ESWs; this knowledge was not available at the start of drafting the 62792 and is currently not available. Consequently, the ESW is treated as a special type of high-voltage pulse generator. The IEC 62792 allows three levels of measurement systems: a high bandwidth, high resolution primary measurement system for use in a standards/calibration laboratory, a secondary system that must be traceable to the primary system, and a tertiary system that must be traceable to either a secondary or primary system. All waveform parameters that are expected to be important to characterize the ESW electrical output are described and contained in one clause. Another clause is dedicated to the description of measurement system calibration, another to the description of the measurement systems and the performance requirements of its components, and another clause on the measurement process.

Summary

We have described our measurement setup and instrument characterization. We have measured the output of ESWs, the effect of different load resistors, and described some of the parameters that may be useful for future research in the ESWs’ effects on humans. We also describe the efforts to draft a measurement standard for characterizing ESWs.

References

- [1] Nave, C. R., and Nave, B. C., "Physics For the Health Sciences," 3rd Ed, W. B. Saunders, 1985.
- [2] Mittal, S., et. al., "Comparison of a Novel Rectilinear Biphasic Waveform With a Damped Sine Wave Monophasic Waveform for Transthoracic Ventricular Defibrillation," Journal of the American College of Cardiology, Vol. 34, No. 5, pp. 1595–601, 1999
- [3] IEC CEI TS 60479-2:2007, Effects of Current on Human Beings and Livestock – Part 2: Special Aspects.
- [4] Gabriel, C., and Gabriel, S., "Compilation Of The Dielectric Properties Of Body Tissues At RF And Microwave Frequencies," Final Report for the Period 15 December 1994 - 14 December 1995, Prepared for AFOSR/NL Bolling AFB DC 20332-0001. See also <http://niremf.ifac.cnr.it/docs/DIELECTRIC/Report.html#Introduction> (accessed 4/42013).
- [5] Gowrishankar, T. R., Pliquett, U., Weaver, J. C., "Changes in Skin Structure and Electrical Properties following High Voltage Exposure," Annals of NY Academy of Sciences, Vol. 888, Nov 1999, pp183-194.
- [6] Panescu, D., "Design and Medical Safety of Neuromuscular Incapacitation Devices," IEEE Engineering in Medicine and Biology Magazine, Sep/Oct 2007, pp 57-67.
- [7] Rahmati, P., Dawson, D., and Adler, A., "Towards a Portable, Memory-Efficient Test System for Conducted Energy Weapons," 24th Canadian Conference on Electrical and Computer Engineering (CCECE), Niagra Falls, Canada, 2011 , pp: 956 – 960.
- [8] Baker-Jarvis, J., Kaiser, R., Janezic, M. D., "Phantom Materials Used To Model Detection Of Concealed Weapons And Effects On Implant Devices In Metal Detectors," URSI 2002, XXVIIth General Assembly of the International Union of Radio Science, Aug 17-24, 2002, Maastricht, Netherlands.
- [9] Dawson, D., Maimaitijiang, Y., Adler, A., "Development of a performance calibration system for X-26 tasers," Medical Measurements and Applications Proceedings (MeMeA), 2010 IEEE International Workshop on, pp: 107 – 112.
- [10] Paulter, Jr., N. G., and Larson, D. R., "Pulse parameter uncertainty analysis," Metrologia, 39(2), 143-155, 2002.
- [11] Souders, T. M., Waltrip, B. C., Laug, O. B., and Deyst, J. P., "A Wideband Sampling Voltmeter IEEE Trans. on Instrum. Meas., Vol. 46, No. 4, pp. 947-953, Aug. 1997.
- [12] Stenbakken, G. N., and Deyst, J. P., "Time-base nonlinearity determination using iterated sine-fit analysis," IEEE Trans. Instrum. Meas. 47(5), pp 1056-1061, 1998.
- [13] IEEE Std 4-1995 "IEEE Standard Techniques for High-Voltage Testing." (New York).
- [14] IEEE Standard on Transitions, Pulses, and Related Waveforms, IEEE Std 181-2003 (New York).